energies

MDPI

Article

Impact of Influent Composition and Operating Conditions on Carbon and Nitrogen Removal from Urban Wastewater in a Continuous-Upflow (Micro)Aerobic Granular Sludge Blanket Reactor

Anna Lanzetta [1,*], Francesco Di Capua [2], Balamurugan Panneerselvam [3], Davide Mattioli [4], Giovanni Esposito [1] and Stefano Papirio [1]

[1] Department of Civil, Architectural and Environmental Engineering, University of Naples Federico II, Via Claudio 21, 80125 Naples, Italy; giovanni.esposito1@unina.it (G.E.); stefano.papirio@unina.it (S.P.)
[2] School of Engineering, University of Basilicata, via dell'Ateneo Lucano 10, 85100 Potenza, Italy; francesco.dicapua@unibas.it
[3] Department of Community Medicine, Saveetha Medical College, SIMATS, Chennai 602105, India; balamurugan.phd10@gmail.com
[4] Laboratory Technologies for the Efficient Use and Management of Water and Wastewater, Italian National Agency for New Technologies, Energy and Sustainable Economic Development (ENEA), Via M.M. Sole 4, 40129 Bologna, Italy; davide.mattioli@enea.it
* Correspondence: anna.lanzetta@unina.it; Tel.: +39-3382829137

Abstract: Aerobic granular sludge is an interesting alternative to the conventional activated sludge (CAS) system and modified-Ludzack–Ettinger (MLE) process for biological wastewater treatment, as it allows a more cost-effective and simultaneous removal of carbon (C) and nitrogen (N) compounds in a single stage. In this study, (micro)aerobic C and N removal from synthetic urban wastewater was investigated in a continuous-double-column-upflow aerobic granular sludge blanket (UAGSB) system. The UAGSB reactor was operated under different dissolved oxygen (DO) ranges (0.01–6.00 mg·L^{-1}), feed C/N ratios (4.7–13.6), and hydraulic retention times (HRTs) (6–24 h). At a DO range of 0.01–0.30 mg·L^{-1}, feed C/N ratio of 13.6, and HRT of 24 h, the UAGSB achieved the highest chemical oxygen demand (COD), N-NH_4^+, and total inorganic nitrogen (TIN) removal efficiencies of 86, 99, and 84%, respectively. A preliminary assessment of the energy and economic savings associated with the process investigated was also carried out. The impact of capital and operating costs mainly related to the energy consumption of the aeration was taken into account. The assessment reveals that the capital and energy expenses of the UAGSB reactor would result in cost savings of around 14 and 7%, respectively, compared with a MLE system.

Keywords: aerobic granular sludge; urban wastewater; carbon and nitrogen removal; simultaneous nitrification and denitrification; microaerobic conditions; energy saving

Citation: Lanzetta, A.; Di Capua, F.; Panneerselvam, B.; Mattioli, D.; Esposito, G.; Papirio, S. Impact of Influent Composition and Operating Conditions on Carbon and Nitrogen Removal from Urban Wastewater in a Continuous-Upflow (Micro)Aerobic Granular Sludge Blanket Reactor. *Energies* **2023**, *16*, 6303. https://doi.org/10.3390/en16176303

Academic Editor: Antonio Zuorro

Received: 8 August 2023
Revised: 25 August 2023
Accepted: 28 August 2023
Published: 30 August 2023

1. Introduction

In the last decades, the increasing urbanization and industrialization have caused an increase in wastewater production and discharge of carbonaceous and nitrogenous compounds, especially in developing countries, leading to oxygen depletion and eutrophication in surface waters [1]. Biological processes in wastewater treatment plants (WWTPs) are often performed within conventional activated sludge (CAS) systems for the removal of organic matter and within the modified Ludzack–Ettinger (MLE) process, consisting of separate denitrification and nitrification steps, for combined carbon (C) and nitrogen (N) removal. However, current research is looking for alternative solutions to improve treatment efficiencies, while minimizing capital and operational costs [2].

In this regard, the simultaneous nitrification and denitrification process (SND) is one of the promising alternatives to the MLE cycle in WWTPs for the treatment of urban wastewaters due to the lower carbon demand for denitrification and reduced sludge production [3], lower energy for aeration [4], and smaller footprint [5]. Specifically, SND is capable of completely removing N in a single-stage system under specific operating conditions, thus, differently from what occurs in MLE systems. The SND process is affected by environmental and operating factors, such as the pH, temperature, dissolved oxygen (DO), hydraulic retention time (HRT), feed carbon-to-nitrogen (C/N) ratio, diffusion limitations inside flocs or biofilm, microbial competition, and type of influent wastewater [6]. These factors play an essential role in regulating the balance among the different bacterial communities, as well as the process efficiency [5,7].

Up to now, processes allowing the concomitant removal of C and N, such as SND, have been investigated in different bioreactor configurations, such as the sequencing batch reactor (SBR) [6,8], moving bed SBR (MBSBR) [9], sequencing batch biofilm reactor (SBBR) [10], moving bed biofilm reactor (MBBR) [11], and aerobic granular sludge (AGS) system [5,6]. Generally, the use of biofilm-based systems promotes the coexistence of different microbial communities and allows the higher concentration of active biomass, while reducing space requirements and sludge production compared to suspended-floc systems, such as CAS and MLE [12]. AGS integrates the characteristics of suspended-growth and biofilm systems, as it leads to the formation of microbial aggregates without any support and having a structure similar to biofilms [13]. The different DO gradients and redox profiles within the aerobic granules result in the formation of (micro)aerobic, anoxic, and anaerobic zones, promoting the coexistence of nitrifiers, denitrifiers, and anaerobic organic-degrading bacteria [14], respectively, and enabling concomitant organics and nutrients removal [6].

Granular sludge was first discovered in upflow anaerobic sludge blanket (UASB) systems in the 1980s [15] and has mainly been employed for anaerobic digestion [16] or removal of oxyanions under anoxic conditions [17]. At the end of 1980s, granular sludge was also applied in aerobic reactors to cope with high organic and nutrient loads [18]. Although aerobic granules were first reported in a continuous-upflow aerobic granular sludge blanket (UAGSB) system [6,19], in recent years, AGS has mainly been cultivated in SBRs and stood out as a reliable technology at the laboratory [13], pilot [20], and full scale [21]. Nonetheless, a continuous-flow AGS system might be advantageous over SBRs for large-scale operations due to the lower installation costs and easier operation, maintenance, and control [3,15]. However, one of the main challenges for an effective continuous-flow AGS operation is the long-term physical stability of the granules, which is affected by several factors, such as the C/N ratio and aeration intensity, as well as the organic and nitrogen loading rates [22]. Hence, a fundamental aspect to be further investigated in continuous-flow AGS systems is represented by C and N removal at different DO concentrations, feed C/N ratios, and HRTs [23]. A proper DO control strategy is a requirement for the selection and maintenance of key bacteria for the SND process, such as ammonia oxidizing bacteria (AOB) and nitrite oxidizing bacteria (NOB) [24]. Decreasing aeration requirements for wastewater treatment is crucial to limit the carbon footprint and operational costs of WWTPs. In fact, studies have shown that aeration system energy consumption can account for 30–76% of the total energy consumption in sewage treatment plants [25–30].

Moreover, the wastewater composition and HRT can strongly influence the performance of continuous-flow AGS systems, and their influence under different DO conditions should be assessed. Typically, high C/N ratios (>10) are beneficial for the long-term operation of AGS systems in terms of both the granular integrity and efficiency [31]. The HRT of continuous-flow AGS should be chosen appropriately to avoid the wash-out of the granules and system instability [32,33].

Although the use of continuous-flow conditions in AGS systems has been reported to make granulation less favorable, the good performance and properties of this technology,

along with the fact that most large-scale plants are operated in a continuous mode, encourage further research and development [34]. Only a few studies have focused on defining optimal operating conditions to achieve high removal efficiencies in terms of organic matter and nitrogen (Table 1). Also, previous continuous-flow AGS bioreactor experiences lasted less than 100 d [35], indicating that limited information regarding long-term AGS bioreactor operations can be drawn. Studies assessing the influence of different operating conditions and long-term operation on the system performance are necessary to promote large-scale application, while trying to reduce the operating costs for urban wastewater treatment.

Table 1. COD, TIN, and N-NH_4^+ REs for synthetic and real urban wastewater in continuous-flow aerobic and anaerobic granular sludge reactors.

Urban Wastewater Characteristics		Reactor Configuration	Process Conditions	Scale	NH_4^+-N RE (%)	COD RE (%)	TN RE (%)	Reference
Synthetic	COD = 144–628 mg·L^{-1} N-NH_4^+ = 20–72 mg·L^{-1}	Micro-aerobic granular sludge reactor	DO_{influx} = 0.11–0.25 g·L^{-1}·d^{-1} HRT = 5–10 h	Lab-scale, V = 18 L	40–86	93–95	51–82	[31]
Real	COD = 150–300 mg·L^{-1}	UASB	HRT = 10–48 h T= 20 °C	Lab-scale, V = 8 L	/	82–86	/	[32]
Real	COD = 602–866 mg·L^{-1} N-NH_4^+ = 48 mg·L^{-1}	UASB	HRT = 8.8–24 h T = 25–30 °C	Pilot-scale, V = 2.75 m^3	/	60 (as sCOD)	/	[33]
Real	COD = 450–8150 mg·L^{-1} N-NH_3^+ = 31.2–141.9 mg·L^{-1}	UASB	HRT = 24.85–106.85 h T = 22.4–30.7 °C	Real-scale, 7800 m^3	/	45–88	25.3	[34]
Synthetic	COD = 500 mg·L^{-1} TN = 50–56 mg·L^{-1}	UASB	HRT = 9–22 h T = 25–35 °C	Lab-scale, V = 0.9 L	/	84–94	<73	[35]
Synthetic	N-NH_4^+ = 512–594 mg·L^{-1}	Continuous-flow airlift reactor (ALR)	HRT = 5.41–22.8 h	Lab-scale, V = 9.2 L	94.4–100	/	/	[36]
Synthetic	Organic loading rate (OLR) = 7.0 kg COD·m^{-3}·d^{-1} N-NH_4^+ * = 21 mg·L^{-1} *	Continuous-flow aerobic granular sludge reactor	HRT = 24 h	Lab-scale, V= 6.8 L	/	83–84	/	[37]
Real	COD = 200–400 mg·L^{-1} N-NH_4^+ = 30–40 mg·L^{-1}	Modified oxidation ditch (MOD)	HRT = 3 h	Lab-scale, V = 60 L	95	90 (as BOD_5)	/	[21]
Synthetic	COD * = 514 mg·L^{-1} N-NH_4^+ * = 63 mg·L^{-1}	Continuous-flow aerobic granular sludge reactor	DO = 0.3–3.5 mg O_2·L^{-1} HRT = 10 h	Lab-scale, V = 890 mL	/	85	/	[38]
Synthetic	COD = 350–1500 mg·L^{-1} N-NH_4^+ * = 53.3 mg·L^{-1}	Continuous-flow aerobic granular sludge reactor	DO = 7.0 mg O_2·L^{-1}	Lab-scale V= 11.9 L	6–60	90–97	/	[39]
Synthetic	COD = 195–604 mg·L^{-1} N-NH_4^+ = 37.9–45.3 mg·L^{-1}	Continuous-upflow aerobic granular sludge blanket	DO = 0.01–6.0 mg O_2·L^{-1} C/N = 4.7–13.5 HRT = 6–24 h	Lab-scale, V = 600 mL	63–100	61–88	28–88 (as TIN)	This study

* Stoichiometrically calculated.

Hence, in this work, the performance of a continuous-flow double-column UAGSB reactor was studied for a period of 306 days to investigate the effect of different DO concentrations, feed C/N ratios, and HRTs on the COD, N-NH_4^+, and total inorganic nitrogen (TIN) removal, as well as on the evolution of the different N species. Batch activity tests were also run to assess the denitrification activity in the bioreactor. Moreover, a first estimation of the capital and operating costs associated with the UAGSB reactor was performed to better evaluate whether the process could result in economic savings as compared to an MLE system.

2. Materials and Methods

2.1. Wastewater Composition and Source of Inoculum

The synthetic wastewater used as influent for the UAGSB reactor was prepared by using two different liquid media (A and B) [40], a trace element solution [41] and tap water. Medium A was composed of 3.32–13.3 g·L^{-1} of sodium acetate trihydrate ($CH_3COONa·3H_2O$) as the organic carbon source and 0.912 g·L^{-1} of magnesium sulfate ep-

tahydrate ($MgSO_4 \cdot 7H_2O$). Medium B contained 1.98 $g \cdot L^{-1}$ of ammonium chloride (NH_4Cl) as the N-NH_4^+ source, 0.555–5.226 $g \cdot L^{-1}$ of dipotassium hydrogen phosphate (K_2HPO_4) as the P-PO_4^{3-} source, and 0.175 $g \cdot L^{-1}$ of potassium chloride (KCl). The influent was prepared by mixing 150 mL of medium A, 150 mL of medium B, 10 mL of trace element solution, and 1300 mL of tap water. Acetate supplementation was varied along the study, resulting in an influent COD concentration ranging from 195 to 617 mg $COD \cdot L^{-1}$ and a feed C/N ratio ranging from 4.7 to 13.6 (Table 2). Furthermore, the feed phosphorus (P) concentration was maintained in the range of 56.4–79.4 $mg \cdot L^{-1}$ (on average) during the batch phase and the first period of the continuous phase to stimulate biomass growth, while lower P concentrations in the range of 6.7–11.8 $mg \cdot L^{-1}$ were maintained in the feed during the remaining periods to simulate P levels in a real municipal wastewater system (Table 2). The influent NH_4^+ concentration was maintained stable throughout the UAGSB operation at a value of 40.7 ± 5.0 mg $N \cdot L^{-1}$. The inoculum used for the start-up of the bioreactor was composed of AGS collected from a 1 L lab-scale SBR operated by Sguanci et al. [42].

Table 2. Operating conditions and duration of each experimental period during the continuous-flow operation of the UAGSB reactor.

Period	Duration (days)	DO Range ($mg \cdot L^{-1}$)	HRT (h)	Feed P-PO_4^{3-} ($mg \cdot L^{-1}$)	Feed COD ($mg \cdot L^{-1}$)	Feed N-NH_4^+ ($mg \cdot L^{-1}$)	Feed C/N
I	0–30	4.0–6.0	24	56.4 ± 25.0	552 ± 55	38.8 ± 6.4	12.1 ± 1.4
II	31–37	2.0–4.0	24	7.5 ± 1.8	604 ± 62	45.3 ± 2.5	13.3 ± 1.4
III	38–65	1.0–2.0	24	8.2 ± 4.8	543 ± 47	43.3 ± 2.9	12.7 ± 1.5
IV	66–87	0.02–1.60	24	6.6 ± 3.1	571 ± 45	42.6 ± 4.3	13.5 ± 1.4
V	88–130	0.12–2.09	24	8.7 ± 3.1	287 ± 141	39.9 ± 8.5	7.0 ± 2.5
VI	131–160	0.10–2.07	24	6.7 ± 2.2	195 ± 30	42.1 ± 2.0	4.7 ± 0.9
VII	161–193	0.03–1.86	24	9.7 ± 2.7	324 ± 47	40.8 ± 2.2	8.0 ± 1.1
VIII	194–220	0.01–0.30	24	10.5 ± 2.9	560 ± 80	41.5 ± 4.3	13.6 ± 2.2
IX	221–258	0.01–1.22	12	12.7 ± 3.6	472 ± 54	41.4 ± 2.1	11.4 ± 1.4
X	259–306	0.01–0.07	6	10.5 ± 1.8	455 ± 30	37.9 ± 3.3	12.1 ± 1.2

2.2. Experimental Set-up

As shown in Figure 1, the experimental set-up included two laboratory-scale glass columns (0.6 L each), one used as the main bioreactor and the other as an aeration column. A 205S peristaltic pump (Watson-Marlow, Falmouth, Cornwall, UK) was used for influent feeding and effluent suction from the bioreactor. The aeration was performed in a separate column to avoid the loss of biomass from the top of the reactor and prevent damaging of the granules due to impact with air bubbles [43]. The effluent from the bioreactor was oxygenated in the aeration column and recirculated at the bottom of the bioreactor with a 505U peristaltic pump (Watson-Marlow, UK) at a flow rate between 20 and 40 $mL \cdot min^{-1}$. Air was transferred to the aeration column at a flow rate ranging from 0 to 4.5 $L \cdot min^{-1}$ using an aquarium air pump equipped with tubing and a porous stone. DO was monitored twice a day and maintained at different ranges by manually adjusting the air flow during the initial batch phase and the first three experimental continuous-flow periods. Successively, the DO concentration was controlled and monitored continuously. Monitoring was performed using a FDO 925 optical probe (WTW, Oberbayern, Germany) connected to a multiparameter benchtop meter, inoLab® Multi 9620 IDS (WTW, Oberbayern, Germany). A Raspberry PI 3 Model B+ single-board computer (Raspberry Pi Foundation, Cambridge, UK) coupled with Python software 3.0 (Python Software Foundation, Wilmington, DE, USA) was used to control and automate aeration in the reactor, as described by Iannacone et al. [44]. The portable DO meter was connected via a USB port to the Raspberry PI, which was programmed to switch on and off a 5 V relay connected to the air pump at fixed DO values. Temperature was not controlled during the study to simulate real operating conditions and remained in the range of 14.0–26.5 °C during period I-VI, 20.3–30.5 °C during period VII-IX, and 16.8–28.5 °C during period X.

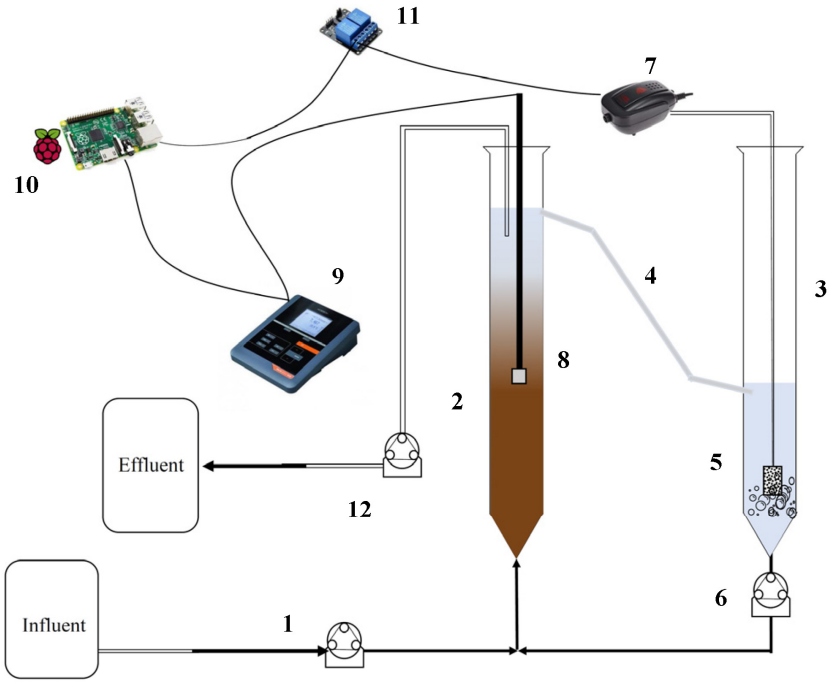

Figure 1. Schematic diagram of the UAGSB reactor configuration: (1) inlet pump; (2) bioreactor; (3) aeration column; (4) effluent recirculation; (5) air sparger; (6) recirculation pump; (7) aquarium air pump; (8) DO probe; (9) oxygen benchtop meter; (10) Raspberry PI 3 Model B^+; (11) relay 5V; (12) effluent pump.

2.3. Experimental Design

The bioreactor was operated for 21 days in batch mode to promote the acclimation and reactivation of the inoculated AGS biomass. Half of the solution was replaced with fresh synthetic wastewater as soon as the COD and NH_4^+ were completely consumed. In this phase, the DO concentration was monitored twice a day and ranged between 3.0 and 4.0 mg·L^{-1}. Subsequently, the bioreactor was operated in continuous mode for 306 days, divided into 10 experimental periods, which are outlined in Table 2. During the first four periods (days 0–87), the DO concentration was progressively reduced from 5.0 to 0.8 mg·L^{-1} (average values) to investigate the impact of reduced oxygenation on organic carbon and TIN removal in the UAGSB reactor. From period V (days 88–130) to VIII (days 194–220), the DO concentration was maintained between 0.03 and 2.09 mg·L^{-1}, and the influence of different feed C/N ratios (4.7, 6.9, 7.9, and 13.6 on average) on the system was evaluated. During periods IX and X (days 221–306), the DO range and feed C/N ratio were maintained between 0.01 and 1.22 mg·L^{-1} and 11.8 ± 1.4, respectively, while the HRT was decreased from 24 (periods I–VIII) to 12 (period IX) and 6 h (period X) to investigate the reactor response to increasing organic and N loads.

2.4. Anoxic Batch Activity Test

A batch activity test was carried out at the end of period IV to assess the denitrifying activity of the biomass populating the bioreactor [45]. The test was performed in triplicate in 250 mL serum bottles at 20 °C by using a medium composed of NO_3^- (100 mg·L^{-1}), sodium acetate trihydrate (600 mg·L^{-1}), and nutrients, as in the UAGSB reactor influent. Prior to starting the experiment, each bottle was flushed with argon gas for 30 s to ensure anoxic conditions. Mixing was provided by a tilting shaker working at a speed of 300 rpm. The N-NO_3^- and N-NO_2^- concentrations were monitored for 3 h, with a sampling interval of 15 min during the first hour and 30 min during the remaining time.

2.5. Calculations

The removal efficiencies (REs) of N-NH_4^+, COD, and TIN; the percentage of total influent nitrogen used for biomass growth ($TIN_{inf,G}$); the percentage of removed inorganic nitrogen used for biomass growth ($TIN_{rem,G}$); and the percentage of total influent inorganic nitrogen being denitrified (TIN_{den}) were calculated by using the following Equations (Equations (1)–(6)):

$$N{-}NH_{4\ RE}^{+} = \frac{\left(\left[N{-}NH_{4\ INF}^{+}\right] - \left[N{-}NH_{4\ EFF}^{+}\right]\right)}{\left(\left[N{-}NH_{4\ INF}^{+}\right]\right)} \times 100 \quad (1)$$

$$COD_{RE} = \frac{\left(\left[COD_{IN}\right] - \left[COD_{EFF}\right]\right)}{\left(\left[COD_{INF}\right]\right)} \times 100 \quad (2)$$

$$TIN_{RE} = \frac{\left(\left[N{-}NH_{4\ INF}^{+}\right]+\left[N{-}NO_{3\ INF}^{-}\right]+\left[N{-}NO_{2\ INF}^{-}\right]-\left[N{-}NH_{4\ EFF}^{+}\right]-\left[N{-}NO_{3\ EFF}^{-}\right]-\left[N{-}NO_{2\ EFF}^{-}\right]\right)}{\left(\left[N{-}NH_{4\ INF}^{+}\right]+\left[N{-}NO_{3\ INF}^{-}\right]+\left[N{-}NO_{2\ INF}^{-}\right]\right)} \times 100 \quad (3)$$

$$TIN_{inf,G} = \frac{0.05 \times \left(\left[COD_{INF}\right] - \left[COD_{EFF}\right]\right)}{\left(\left[N{-}NH_{4\ INF}^{+}\right] + \left[N{-}NO_{3\ INF}^{-}\right] + \left[N{-}NO_{2\ INF}^{-}\right]\right)} \times 100 \quad (4)$$

$$TIN_{rem,G} = \frac{0.05 \times \left(\left[COD_{INF}\right]-\left[COD_{EFF}\right]\right)}{\left(\left[N{-}NH_{4\ INF}^{+}\right]+\left[N{-}NO_{3\ INF}^{-}\right]+\left[N{-}NO_{2\ INF}^{-}\right]-\left[N{-}NH_{4\ EFF}^{+}\right]-\left[N{-}NO_{3\ EFF}^{-}\right]-\left[N{-}NO_{2\ EFF}^{-}\right]\right)} \times 100 \quad (5)$$

$$TIN_{den} = \left[TIN_{RE} - TIN_{inf,G}\right] \quad (6)$$

where:

- [N-$NH_4^+{}_{INF}$] and [N-$NH_4^+{}_{EFF}$] are the influent and effluent N-NH_4^+ concentrations, respectively;
- [COD_{INF}] and [COD_{EFF}] are the influent and effluent COD concentrations, respectively;
- [N-$NO_X^-{}_{INF}$] and [N-$NO_X^-{}_{EFF}$] are the influent and effluent N-NO_X^- (nitrate- and nitrite-nitrogen) concentrations, respectively.

2.6. Analytical Methods

Liquid samples were collected daily from the UAGSB reactor and filtered through 0.45 µm syringe filters with polypropylene membranes (VWR, USA) prior to analysis. The COD concentration was determined by the closed reflux colorimetric method [46]. The NH_4^+ concentration was determined spectrophotometrically using the indophenol blue method [47]. DO, pH, NO_3^-, and NO_2^- concentrations were measured as described by Di Capua et al. [48]. Total suspended solids (TSSs) and volatile suspended solids (VSSs) concentrations were analyzed according to the Standard Methods [46].

2.7. Energy and Economic Assessment of the UAGSB Reactor

To assess the potential energetic and economic benefits of the UAGSB reactor, this was compared with a MLE system, considering for the latter only the denitrification and nitrification steps and assuming to serve a population equivalent (PE) of 10,000 inhabitants for both systems. The operating conditions experimentally identified as the best performing in this study were used to size the UAGSB and MLE systems. The volume of the nitrification (V_N) and denitrification (V_D) tanks of the MLE system, the oxygen demand (OD) of nitrification, the operative oxygen capacity (OC), and the number of air diffusers for both plants were calculated as reported by Bonomo [49]. A DO concentration of 2.0 mg·L^{-1} was considered for the MLE system [50], while a DO concentration equal to the upper value of the DO interval of period VIII was used for the UAGSB reactor. The

capital expenditure (CAPEX) was assessed taking into account the following equation (Equation (7)), as reported in the local plans of Campania Region (Italy) [51]:

$$CAPEX\left(EUR{\cdot}\mathrm{PE}^{-1}\right) = 178.45\ PE^{-0.282} \quad (7)$$

Operational costs were based on the power use of aerators, considering the technical data of a commercial ceramic disc diffuser produced by Xylem Inc. (Hong Kong, China) The energy consumption associated with aeration was calculated based on the OD of the nitrification process and the standard aeration efficiency (SAE) of the selected aerators, assuming a continuous aeration in the system, as reported in Equation (8).

$$Aeration\ energy\ consumption\left(\mathrm{kWh}{\cdot}\mathrm{year}^{-1}\right) = \frac{OD}{SAE} \quad (8)$$

2.8. Statistical Data Analysis

A one-way analysis of variance (ANOVA) was performed for data analysis, using the Data Analysis Tool of Excel 2016 (Microsoft Corporation, Redmond, WA, USA). The ANOVA was conducted to determine the statistical differences in the performance parameters in terms of COD, N-NH_4^+, and TIN removal. The significant difference was set at 95% ($p < 0.05$).

3. Results and Discussion

3.1. Effect of DO Concentration on COD and N Removal Efficiencies of the UAGSB Reactor

The first four periods were aimed at evaluating the effect of different DO concentrations on the REs of COD, N-NH_4^+, and TIN at feed C/N ratios in the range of 12.1–13.5 (Table 2). The decrease in the DO concentration from period I (4.0–6.0 mg·L^{-1}) to period IV (0.02–1.60 mg·L^{-1}) resulted in stable ($p > 0.05$) N-NH_4^+ and TIN REs of 95 ± 9 and 85 ± 8% (Table 3), respectively, with a maximum effluent N-NO_3^- concentration of 10.6 mg·L^{-1}. Additionally, the DO decrease did not negatively affect the COD RE, which remained stable at 84 ± 5% ($p > 0.05$) in the first four periods (Table 3), indicating that the UAGSB reactor could be efficiently operated at low DO conditions, thus entailing low aeration costs for the treatment of wastewater.

Table 3. COD, TIN, and N-NH_4^+ REs obtained in the UAGSB reactor at different DO concentrations (periods I-IV), C/N ratios (periods V-VIII), and HRTs (periods IX-X). The percentages of total influent and removed nitrogen used for biomass growth ($TIN_{inf,G}$ and $TIN_{rem,G}$, respectively) and of total influent inorganic nitrogen being denitrified (TIN_{den}) were calculated considering a COD:N ratio of 100:5 for aerobic cell synthesis.

Period	NH_4^+-N RE (%)	TIN RE (%)	COD RE (%)	$TIN_{INF,G}$ (%)	$TIN_{REM,G}$ (%)	TIN_{DEN} (%)
I	93 ± 12	83 ± 12	85 ± 1	46 ± 5	60 ± 8	32 ± 8
II	100 ± 0	88 ± 2	78 ± 4	47 ± 4	54 ± 5	40 ± 5
III	95 ± 6	85 ± 5	84 ± 5	48 ± 7	51 ± 21	42 ± 16
IV	94 ± 8	82 ± 6	88 ± 1	52 ± 5	63 ± 8	30 ± 8
V	97 ± 5	64 ± 19	61 ± 16	20 ± 10	30 ± 15	45 ± 15
VI	99 ± 2	28 ± 8	63 ± 7	14 ± 4	53 ± 18	14 ± 8
VII	97 ± 6	61 ± 12	74 ± 4	28 ± 4	47 ± 12	34 ± 13
VIII	99 ± 2	84 ± 12	86 ± 3	55 ± 9	67 ± 15	29 ± 15
IX	90 ± 13	77 ± 10	75 ± 6	40 ± 6	53 ± 11	37 ± 12
X	63 ± 18	64 ± 15	71 ± 8	41 ± 6	68 ± 10	21 ± 10

In a previous study, Liu and Dong [52] observed that reducing the oxygen flow from 0.25 to 0.11 $g \cdot L^{-1} \cdot d^{-1}$ in a continuous-flow AGS system resulted in a decrease in N-NH_4^+ and TIN REs of about 46 and 31%, respectively. This was ascribed to an enhanced competition for DO between AOB and heterotrophic organisms in the outer layer of the granules, combined with a decreased depth of oxygen penetration, which resulted in a decreased nitrification efficiency at lower DO values [53,54]. In contrast with Liu and Dong [52], the N-NH_4^+ and TIN removals were not impaired at decreasing DO concentrations in the UAGSB reactor run in this study. However, it should be pointed out that, according to our calculations, about half of the feed N was removed via biomass growth. Indeed, considering a COD:N ratio of 100:5 for aerobic cell synthesis and that the influent COD concentration and feed C/N ratios were, respectively, 565 ± 80 $mg \cdot L^{-1}$ and 12.9 ± 1.5 during periods I-IV, the estimated N uptake for microbial growth ($TIN_{inf,G}$) accounted for 46–52% of the influent TIN (Table 3). This percentage increases if the amount of N taken up for microbial growth is calculated on the removed TIN ($TIN_{rem,G}$), reaching 51–63% (Table 3). The remaining fraction of nitrogen (37–49%) not detected in the effluent was likely removed via SND.

The existence of an active denitrifying community in the granular biomass was confirmed by the anoxic batch activity tests carried out at the end of period IV. A gradual N-NO_3^- reduction was observed over time, with consequent N-NO_2^- build-up and consumption (Figure S1). After 150 min, denitrification ceased, as both NO_3^- and NO_2^- concentrations were below the detection limit. In the UAGSB reactor, the average TIN_{den} calculated in periods I-IV (Equation (6)) was 36% (Table 3), with no significant differences at decreasing DO concentrations ($p > 0.05$), indicating that denitrification also occurred at high oxygen concentrations (DO > 1.60 $mg \cdot L^{-1}$).

As shown in Figure 2, the TSS and VSS concentrations in the UAGSB system at the end of period III (day 56) dropped from 2.5 ± 0.7 to 1.1 ± 0.6 $mg \cdot L^{-1}$ and from 1.7 ± 0.2 to 0.8 ± 0.3 $mg \cdot L^{-1}$, respectively. However, at the end of period IV (day 70), the TSS and VSS concentrations increased up to 2.4 ± 0.3 and 1.1 ± 0.2 $mg \cdot L^{-1}$, respectively, likely due to the biomass adaptation to lower DO conditions.

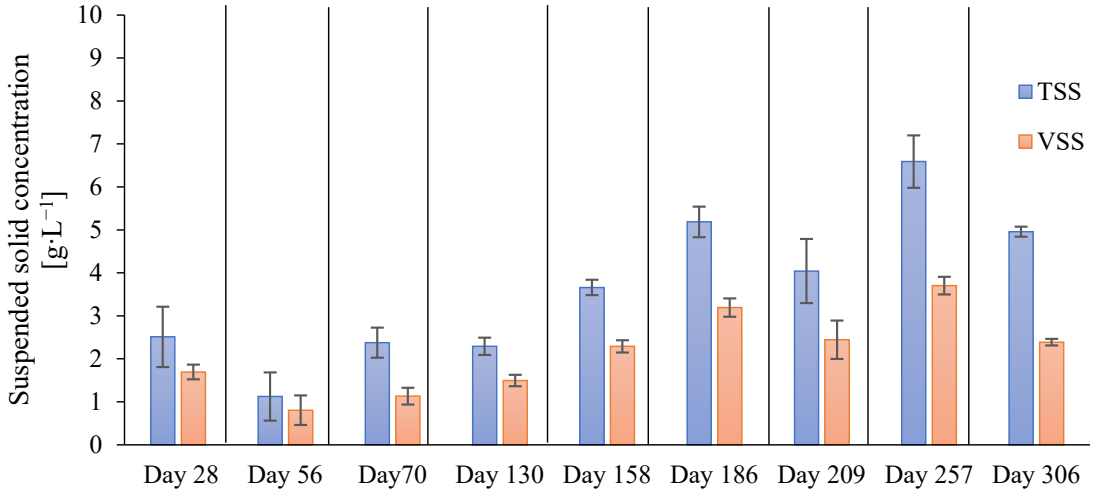

Figure 2. Evolution of the mean total (TSS) and volatile suspended solid (VSS) concentrations along the 306 days of the UAGSB reactor operation.

3.2. Performance of the UAGSB Reactor under Different Feed C/N Ratios

Periods V and VI were characterized by similar DO ranges (Table 2) and a decrease in the feed C/N ratio from 13.5 (period IV) to 7.0 and 4.7, respectively. The decrease in the C/N ratio did not negatively affect the N-NH_4^+ RE, which remained in the range of 97–99% ($p > 0.05$) (Table 3). Nevertheless, the mechanisms contributing to N-NH_4^+ removal varied in comparison to the previous experimental periods. The lower feed

COD concentration during period V decreased $TIN_{inf,G}$ and $TIN_{rem,G}$ to approximately 20 and 30%, respectively, while nitrification was stimulated, as the N-NO_3^- concentration increased from 4.5 ± 2.3 (period IV) to 11.9 ± 5.2 (period V) and 31.1 ± 4.1 (period VI) mg N·L^{-1} (Figure 3), resulting in TIN_{den} values of 45% in period V and 14% in period VI (Table 3). On the other hand, the reduction in the feed C/N ratio led to insufficient organic carbon to support denitrification, as also reported by Iannacone et al. [44]. Consequently, the TIN RE reached a minimum value of 28 ± 8% in period VI (Table 3) as a consequence of the increased N-NO_3^- concentrations in the effluent. In contrast, Campo et al. [55] and Wang et al. [56] reported considerably higher TIN REs of about 71 and 78%, respectively, at feed C/N ratios of 3.8 and 3.5 in SBR, which could be due to the sequence of anaerobic and aerobic phases enhancing the selection and activity of functional microorganisms.

The COD RE decreased from 84 ± 5% (periods I–IV) to 62 ± 13% (periods V–VI) (Table 3), while the effluent COD concentration did not change significantly ($p > 0.05$) and stayed at 94.7 ± 55.6 mg·L^{-1} (Figure 4). Biomass growth in the system was not affected by the lower COD levels in the feed, as the TSS and VSS concentrations did not change significantly ($p > 0.05$) in period V and even increased in period VI, reaching 3.66 ± 0.18 mg TSS·L^{-1} and 2.29 ± 0.14 mg VSS·L^{-1}, respectively (Figure 2).

Periods VII and VIII were characterized by an increase in the feed COD concentration and, therefore, of the C/N ratio from 4.7 (period VI) to 8.0 and 13.6, respectively. The increase in the feed COD led to lower DO concentrations in the bioreactor (below 1 mg·L^{-1} in period VIII), even though the inlet air flow rate was increased. Interestingly, despite the low DO conditions, N-NH_4^+ RE was not affected ($p > 0.05$) and remained stable at 98 ± 5%. In period VIII, more than 50% of the influent TIN was used for the biomass growth (Table 3). As expected, the feed C/N increase resulted in a gradual reduction of the effluent N-NO_3^- concentration to an average value of 5.30 mg N·L^{-1} in period VIII, suggesting an increase in the denitrifying efficiency of the system that could be favored by the low DO levels in the bioreactor. TIN_{den} increased from 14% in period VI to 34 and 29% in periods VII and VIII, respectively. However, a gradual increase in the N-NO_2^- concentration up to a value of 3.69 mg N·L^{-1} was observed in period VIII. This suggests that the low DO values probably resulted in a slight inhibition of NOB biomass, leading to NO_2^- build-up in the effluent. The COD RE also increased to 74 ± 4% (period VII) and 86 ± 3% (period VIII) (Table 3). Periods VII-VIII were characterized by a further increase in the TSS and VSS concentrations in the reactor (Figure 2), likely linked to the higher feed COD concentrations stimulating the growth of the heterotrophic families. The results obtained in this stage confirm that the UAGSB reactor is more efficient at higher C/N ratios, even under microaerobic (DO < 1 mg·L^{-1}) conditions, which should be taken into account in view of the future upscaling of the system.

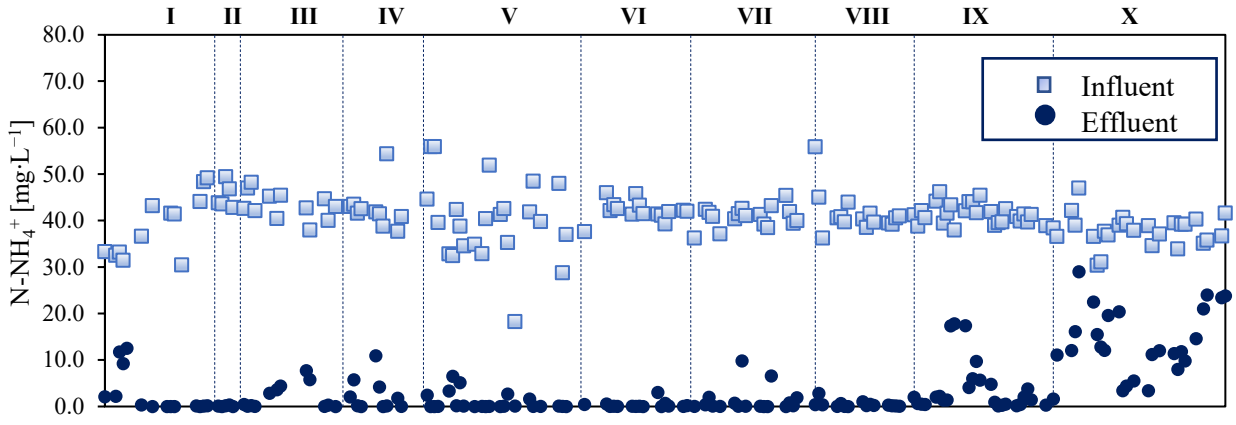

Figure 3. *Cont.*

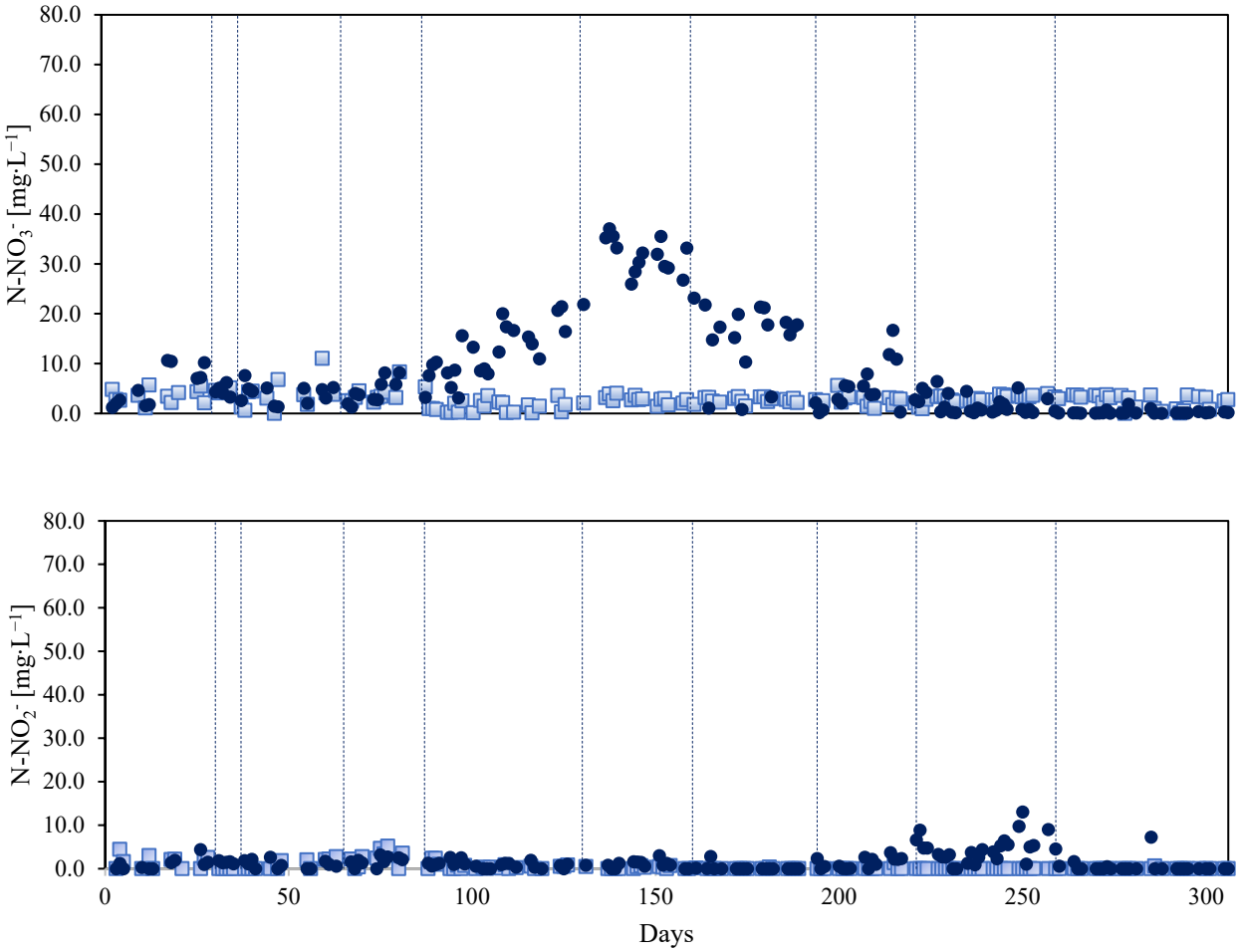

Figure 3. Temporal trend of influent and effluent N-NH_4^+, N-NO_3^-, and N-NO_2^- concentrations (mg·L^{-1}) measured daily along the ten experimental periods of the UAGSB reactor operation.

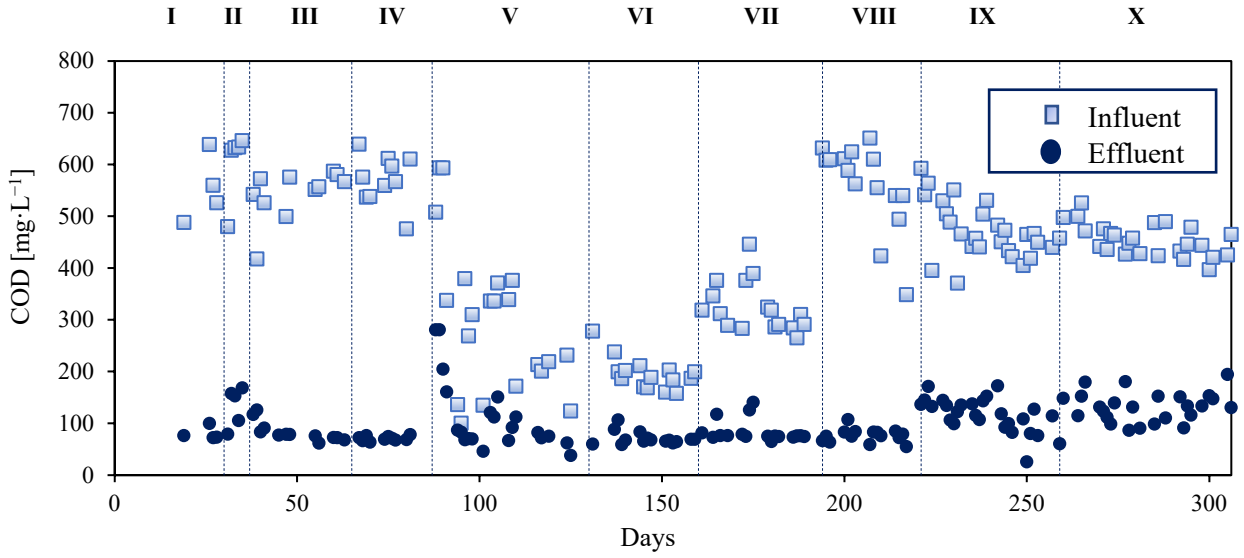

Figure 4. Temporal trend of influent and effluent COD concentrations (mg·L^{-1}) along the ten experimental periods of the UAGSB reactor operation.

3.3. Effect of HRT on the Performance of the UAGSB Reactor

At the beginning of period IX (day 221), the HRT was set at 12 h, with the objective to evaluate the COD, N-NH_4^+, and TIN REs at increased organic and nitrogen loading rates. HRT decrease from 24 to 12 h resulted in a significant decrease in REs ($p < 0.05$). The effluent N-NH_4^+ concentration (Figure 3) abruptly increased shortly after the HRT decrease (day 231) due to a slow biomass adaptation and a period of interruption of the UAGSB reactor operation due to the summer break (Table 3). From day 236 onwards, the N-NH_4^+ RE increased back up to 90 ± 13%. Despite this, a significant increase in the effluent N-NO_2^- concentration was observed, as shown in Figure 3. NO_2^- accumulation indicates that reducing the HRT likely led to partial nitrification, which can be attributed to a reduced contact time between the biomass and influent NH_4^+, as well as to the already limited DO availability in the bioreactor (0.01–1.22 mg·L^{-1}) (Table 2). On the other hand, the low DO levels ensured an elevated TIN_{den} in the bioreactor, being equal to 37% (Table 3). Although lower COD and TIN REs were observed at an HRT of 12 h, the UAGSB performances were still acceptable, being the REs ≥ 75% (on average) and the effluent COD and TIN concentrations often below the effluent standards (COD = 125 mg·L^{-1}, TN = 15 mg·L^{-1}) for safe discharge in water bodies, according to the EU legislation (Council Directive 91/271/EEC) for a population equivalent up to 100,000 inhabitants. At the end of period IX, a significant increase in the TSS and VSS concentrations was observed (Figure 2), which can be attributed to the increased organic loading provided to the system.

In period X (day 259), the HRT was further decreased to 6 h. This led to a gradual reduction of the COD RE to 71 ± 8% (Table 3). Nevertheless, the most important effect of the lower HRT was observed on N-NH_4^+ and TIN REs, which decreased to average values of 63 and 64%, respectively ($p < 0.05$) (Table 3). Therefore, the HRT reduction led to a deterioration of the reactor performance, as also reported by Wan et al. [32]. Considering that the effluent N-NO_3^- and N-NO_2^- concentrations were often negligible, the largest N fraction in the effluent remained as N-NH_4^+ (Figure 3). This suggests that the significant increase in the influent organic and nitrogen loading rates, coupled with the low DO concentrations in the bioreactor, negatively affected nitrification. Consequently, the denitrification performance also drastically decreased, resulting in a TIN_{den} of 21% (Table 3). This period was also characterized by a significant decrease in terms of TSS and VSS concentrations (Figure 2). This was due to sludge washout, which occurred for a period of about two weeks right after the HRT decrease, and the corresponding increase in the influent flow rate, resulting in a biomass loss of about 1.63 g TSS·L^{-1}.

3.4. Preliminary Cost Evaluation

The continuous-flow UAGSB system investigated in this study during period VIII was able to obtain the highest COD, N-NH_4^+, and TIN REs of 86, 99, and 84%, respectively, at a maximum DO concentration of 0.30 mg O_2·L^{-1}, a C/N ratio of 13.6, and an HRT of 24 h. For this reason, the average influent COD and N-NH_4^+ concentrations in period VIII (Table 2) were used to size both the UAGSB reactor and the MLE system. The DO concentration was different between the two systems. The main results obtained are shown in Table 4.

Based on the results of this study, the UAGSB reactor could allow an annual energy saving of about 19,540 kWh·$year^{-1}$. Considering the price of the electric energy as given by the Italian Regulatory Authority for Energy Networks and Environment (ARERA) in July 2023, which is equal to 0.118 EUR·kWh^{-1}, the corresponding economic saving associated is about 2300 EUR·$year^{-1}$. The CAPEX associated with the construction of the MLE and UAGSB systems is about EUR 128,700 and EUR 111,600, respectively (Table 4). By adding the costs of the air diffusers, taking into consideration an approximate cost for each air diffuser of about EUR 19, the total CAPEX of the MLE and UAGSB systems was about EUR 133,800 and EUR 115,400, respectively, with an economic saving of about EUR 18,400. These preliminary economic considerations confirm that the UAGSB system could be a more attractive cost-effective technology than the MLE system.

Table 4. Main results of the preliminary economic evaluation aimed at evaluating the capital (CAPEX) and operating expenses (OPEX) of a UAGSB reactor and a MLE system, both serving a population equivalent (PE) of 10,000 inhabitants.

		MLE	**UAGSB**
Flow rate	$m^3 \cdot year^{-1}$	759,200	759,200
V_N	m^3	1678	2080
V_D	m^3	721	-
OD	$kg\ O_2 \cdot h^{-1}$	79.2	73.6
N. diffusers	-	270	203
Typical standard aeration efficiency (SAE)	$kg\ O_2 \cdot kWh^{-1}$	2.5	2.5
Max. power	$kWh \cdot year^{-1}$	277,560	258,020
Max. energetic costs	**EUR·year^{-1}**	**32,752**	**30,446**
Max. energetic costs	**EUR·m^{-3}**	0.43	0.40
Construction costs	EUR	128,700	111,603
Air diffusers costs	EUR	5097	3820
Total CAPEX	**EUR**	**133,797**	**115,422**

4. Practical Applications and Future Research

The results of this study suggest that the UAGSB reactor can be considered as a promising technology for the simultaneous removal of C and N from wastewaters with C/N ratios as high as 11.4–13.6 when operated at HRT > 6 h. Compared to continuous-flow anaerobic and aerobic granular sludge reactors operated in previous studies (Table 1), the UAGSB reactor herein tested showed comparable or even higher REs under different operating conditions. Further studies should be addressed to a better investigation of the process in the case of low C/N ratios (below 7.0) and HRTs of 6 h or lower, for instance, in the presence of higher biomass concentrations possibly entailing higher REs, and to reduce energy consumption associated with the process. Future research should also focus on the combination of the biological nitrogen removal via SND to P removal in the UAGSB reactor. Moreover, applications of this technology on the pilot- and full-scale would allow for better assessing the effect of the feed wastewater composition on C and N removal and granule stability, as well as for evaluating the associated operating costs.

One drawback of the process that emerged in this study is that the effluent NO_2^- concentration often exceeded the Italian standard (D. Lgs. 152/2006, Annex V, Part III) for industrial wastewater discharge into sewers (0.6 mg $N\text{-}NO_2^-\ L^{-1}$), even under the best operating conditions. Therefore, a post-treatment aiming to reduce NO_2^- levels should be considered. An interesting approach to reduce the residual $N\text{-}NO_3^-$ and $N\text{-}NO_2^-$ concentrations could be the study of a symbiotic process between aerobic granules and microalgae to remove the residual fraction of nitrogen and further reduce the operational costs of the whole process, by using part of the oxygen needed from the microalgal metabolism.

5. Conclusions

The continuous-flow UAGSB system investigated in this study was able to obtain COD, $N\text{-}NH_4^+$, and TIN REs up to 86, 99, and 84%, respectively, at a C/N ratio of 13.6, an HRT of 24 h, and DO concentrations as low as 0.01–0.30 mg $O_2 \cdot L^{-1}$, indicating that bacterial communities playing different roles are properly retained in a single-stage system. Under the best performing conditions, the preliminary cost evaluation showed that the UAGSB reactor could result in a capital and energy cost savings of around 14 and 7%, respectively, compared to a MLE system. Higher effluent COD and $N\text{-}NH_4^+$ concentrations in the UAGSB reactor were observed when decreasing the C/N ratio to 4.7–8.0 and the HRT to 6 h. These results suggest that the use of the UAGSB technology can be highly

recommended, both from an engineering and an economic perspective, for the treatment of urban wastewater, but further research efforts are needed for its validation on a larger scale.

Supplementary Materials: The following supporting information can be downloaded at: https://www.mdpi.com/article/10.3390/en16176303/s1, Figure S1: Temporal trend of N-$NO3^-$ and N-$NO2^-$ concentrations ($mg \cdot L^{-1}$) measured during the anoxic batch activity tests carried out at the end of period IV.

Author Contributions: Conceptualization, A.L., F.D.C., D.M., G.E. and S.P.; Data Curation, A.L.; Formal Analysis, A.L.; Investigation, A.L., F.D.C., B.P. and S.P.; Methodology, A.L., F.D.C., G.E. and S.P.; Visualization, A.L., F.D.C., G.E. and S.P.; Writing—Original Draft Preparation, A.L.; Writing—Review and Editing, A.L., F.D.C., B.P., D.M., G.E. and S.P.; Supervision, F.D.C., D.M., G.E. and S.P.; Project Administration, S.P.; Funding Acquisition, G.E. and S.P. All authors have read and agreed to the published version of the manuscript.

Funding: This work was supported by Programma Operativo Nazionale (PON) FSE-FESR "Ricerca e Innovazione 2014–2020", Azione I.1 "Dottorati Innovativi con caratterizzazione industriale" and by the Project "Energy efficiency of industrial products and processes", Research programme "Piano Triennale della Ricerca del Sistema Elettrico Nazionale 2019–2021" funded by the Italian Ministry of Economic Development.

Data Availability Statement: Not applicable.

Acknowledgments: We would like to thank the Programma Operativo Nazionale (PON) FSE-FESR "Ricerca e Innovazione 2014–2020", Azione I.1 "Dottorati Innovativi con caratterizzazione industriale" for funding the doctoral scholarship of Anna Lanzetta. The authors are also grateful to Anna Esposito and Chiara Maraviglia for their assistance in maintaining the bioreactor.

Conflicts of Interest: The authors declare that they have no known competing financial interest or personal relationships that could have appeared to influence the work reported in this paper.

References

1. Dodds, W.K.; Smith, V.H. Nitrogen, phosphorus, and eutrophication in streams. *Inl. Waters* **2016**, *6*, 155–164. [CrossRef]
2. Bumbac, C.; Ionescu, I.A.; Tiron, O.; Badescu, V.R. Continuous flow aerobic granular sludge reactor for dairy wastewater treatment. *Water Sci. Technol.* **2015**, *71*, 440–445. [CrossRef]
3. Ma, W.; Han, Y.; Ma, W.; Han, H.; Zhu, H.; Xu, C.; Li, K.; Wang, D. Enhanced nitrogen removal from coal gasification wastewater by simultaneous nitrification and denitrification (SND) in an oxygen-limited aeration sequencing batch biofilm reactor. *Bioresour. Technol.* **2017**, *244*, 84–91. [CrossRef] [PubMed]
4. Zinatizadeh, A.A.L.; Ghaytooli, E. Simultaneous nitrogen and carbon removal from wastewater at different operating conditions in a moving bed biofilm reactor (MBBR): Process modeling and optimization. *J. Taiwan Inst. Chem. Eng.* **2015**, *53*, 98–111. [CrossRef]
5. Seifi, M.; Fazaelipoor, M.H. Modeling simultaneous nitrification and denitrification (SND) in a fluidized bed biofilm reactor. *Appl. Math. Model.* **2012**, *36*, 5603–5613. [CrossRef]
6. Di Capua, F.; Iannacone, F.; Sabba, F.; Esposito, G. Simultaneous nitrification–denitrification in biofilm systems for wastewater treatment: Key factors, potential routes, and engineered applications. *Bioresour. Technol.* **2022**, *361*, 127702. [CrossRef]
7. Yan, L.; Zhang, S.; Hao, G.; Zhang, X.; Ren, Y.; Wen, Y.; Guo, Y.; Zhang, Y. Simultaneous nitrification and denitrification by EPSs in aerobic granular sludge enhanced nitrogen removal of ammonium-nitrogen-rich wastewater. *Bioresour. Technol.* **2016**, *202*, 101–106. [CrossRef] [PubMed]
8. Yan, Y.; Lu, H.; Zhang, J.; Zhu, S.; Wang, Y.; Lei, Y.; Zhang, R.; Song, L. Simultaneous heterotrophic nitrification and aerobic denitrification (SND) for nitrogen removal: A review and future perspectives. *Environ. Adv.* **2022**, *9*, 100254. [CrossRef]
9. Wang, J.; Rong, H.; Cao, Y.; Zhang, C. Factors affecting simultaneous nitrification and denitrification (SND) in a moving bed sequencing batch reactor (MBSBR) system as revealed by microbial community structures. *Bioprocess Biosyst. Eng.* **2020**, *43*, 1833–1846. [CrossRef]
10. Chai, H.; Xiang, Y.; Chen, R.; Shao, Z.; Gu, L.; Li, L.; He, Q. Enhanced simultaneous nitrification and denitrification in treating low carbon-to-nitrogen ratio wastewater: Treatment performance and nitrogen removal pathway. *Bioresour. Technol.* **2019**, *280*, 51–58. [CrossRef]
11. Iannacone, F.; Di Capua, F.; Granata, F.; Gargano, R.; Esposito, G. Shortcut nitrification-denitrification and biological phosphorus removal in acetate- and ethanol-fed moving bed biofilm reactors under microaerobic/aerobic conditions. *Bioresour. Technol.* **2021**, *330*, 124958. [CrossRef] [PubMed]

12. Zhao, Y.; Liu, D.; Huang, W.; Yang, Y.; Ji, M.; Nghiem, L.D.; Trinh, Q.T.; Tran, N.H. Insights into biofilm carriers for biological wastewater treatment processes: Current state-of-the-art, challenges, and opportunities. *Bioresour. Technol.* **2019**, *288*, 121619. [CrossRef] [PubMed]
13. Wang, F.; Lu, S.; Wei, Y.; Ji, M. Characteristics of aerobic granule and nitrogen and phosphorus removal in a SBR. *J. Hazard. Mater.* **2009**, *164*, 1223–1227. [CrossRef]
14. Gao, D.; Liu, L.; Liang, H.; Wu, W.M. Aerobic granular sludge: Characterization, mechanism of granulation and application to wastewater treatment. *Crit. Rev. Biotechnol.* **2011**, *31*, 137–152. [CrossRef]
15. Lettinga, G.; van Velsen, A.F.M.; Hobma, S.W.; de Zeeuw, W.; Klapwijk, A. Use of the upflow sludge blanket (USB) reactor concept for biological wastewater treatment, especially for anaerobic treatment. *Biotechnol. Bioeng.* **1980**, *22*, 699–734. [CrossRef]
16. Kumari, K.; Suresh, S.; Arisutha, S.; Sudhakar, K. Anaerobic co-digestion of different wastes in a UASB reactor. *Waste Manag.* **2018**, *77*, 545–554. [CrossRef] [PubMed]
17. Tan, L.C.; Papirio, S.; Luongo, V.; Nancharaiah, Y.V.; Cennamo, P.; Esposito, G.; van Hullebusch, E.D.; Lens, P.N.L. Comparative performance of anaerobic attached biofilm and granular sludge reactors for the treatment of model mine drainage wastewater containing selenate, sulfate and nickel. *Chem. Eng. J.* **2018**, *345*, 545–555. [CrossRef]
18. Shin, H.S.; Lim, K.H.; Park, H.S. Effect of shear stress on granulation in oxygen aerobic upflow sludge bed reactors. *Water Sci. Technol.* **1992**, *26*, 601–605. [CrossRef]
19. Zeng, R.J.; Lemaire, R.; Yuan, Z.; Keller, J. Simultaneous nitrification, denitrification, and phosphorus removal in a lab-scale sequencing batch reactor. *Biotechnol. Bioeng.* **2003**, *84*, 170–178. [CrossRef]
20. Yang, H.G.; Li, J.; Liu, J.; Ding, L.B.; Chen, T.; Huang, G.X.; Shen, J.Y. A case for aerobic sludge granulation: From pilot to full scale. *J. Water Reuse Desalination* **2016**, *6*, 188–194. [CrossRef]
21. Li, J.; Ding, L.; Cai, A.; Huang, G.; Horn, H. Aerobic Sludge Granulation in a Full-Scale Sequencing Batch Reactor. *BioMed Res. Int.* **2014**, *2014*, 268789. [CrossRef] [PubMed]
22. He, Q.; Chen, L.; Zhang, S.; Chen, R.; Wang, H. Bioresource Technology Hydrodynamic shear force shaped the microbial community and function in the aerobic granular sequencing batch reactors for low carbon to nitrogen (C/N) municipal wastewater treatment. *Bioresour. Technol.* **2019**, *271*, 48–58. [CrossRef] [PubMed]
23. De Kreuk, M.K.; Kishida, N.; Loosdrecht, M.C.M. Van Aerobic granular sludge—state of the art. *Water Sci. Technol.* **2007**, *55*, 75–81. [CrossRef] [PubMed]
24. Rosa-masegosa, A.; Muñoz-palazon, B.; Gonzalez-martinez, A.; Fenice, M.; Gorrasi, S.; Gonzalez-lopez, J. New Advances in Aerobic Granular Sludge Technology Using Continuous Flow Reactors: Engineering and Microbiological Aspects. *Water* **2021**, *13*, 1792. [CrossRef]
25. Changqing, L.; Shuai, L.; Feng, Z. The oxygen transfer efficiency and economic cost analysis of aeration system in municipal wastewater treatment plant. *Energy Procedia* **2011**, *5*, 2437–2443. [CrossRef]
26. Campanelli, M.; Foladori, P.; Vaccari, M. *Consumi Elettrici ed Efficienza Energetica nel Trattamento Delle Acque Reflue*; Maggiori Editore: Santarcangelo di Romagna, Italy, 2013; ISBN 8838783683.
27. Gu, Y.; Li, Y.; Yuan, F.; Yang, Q. Optimization and control strategies of aeration in WWTPs: A review. *J. Clean. Prod.* **2023**, *418*, 138008. [CrossRef]
28. Zidan, A.; Nasr, M.; Fujii, M.; Ibrahim, M.G. Environmental and Economic Evaluation of Downflow Hanging Sponge Reactors for Treating High-Strength Organic Wastewater. *Sustainability* **2023**, *15*, 6038. [CrossRef]
29. Dadebo, D.; Ibrahim, M.G.; Fujii, M.; Nasr, M. Sequential treatment of surfactant-laden wastewater using low-cost rice husk ash coagulant and activated carbon: Modeling, optimization, characterization, and techno-economic analysis. *Bioresour. Technol. Rep.* **2023**, *22*, 101464. [CrossRef]
30. Papirio, S.; Esposito, G.; Pirozzi, F. Biological inverse fluidized-bed reactors for the treatment of low pH- and sulphate-containing wastewaters under different COD/SO_4^{2-} conditions. *Environ. Technol.* **2013**, *34*, 1141–1149. [CrossRef]
31. He, Q.; Zhang, W.; Zhang, S.; Wang, H. Enhanced nitrogen removal in an aerobic granular sequencing batch reactor performing simultaneous nitrification, endogenous denitrification and phosphorus removal with low superficial gas velocity. *Chem. Eng. J.* **2017**, *326*, 1223–1231. [CrossRef]
32. Wan, C.; Yang, X.; Lee, D.J.; Sun, S.; Liu, X.; Zhang, P. Influence of hydraulic retention time on partial nitrification of continuous-flow aerobic granular-sludge reactor. *Environ. Technol.* **2014**, *35*, 1760–1765. [CrossRef] [PubMed]
33. Li, J.; Cai, A.; Wang, M.; Ding, L.; Ni, Y. Aerobic granulation in a modified oxidation ditch with an adjustable volume intraclarifier. *Bioresour. Technol.* **2014**, *157*, 351–354. [CrossRef] [PubMed]
34. Kent, T.R.; Bott, C.B.; Wang, Z. State of the art of aerobic granulation in continuous fl ow bioreactors. *Biotechnol. Adv.* **2018**, *36*, 1139–1166. [CrossRef] [PubMed]
35. Xu, D.; Li, J.; Liu, J.; Qu, X.; Ma, H. Advances in continuous flow aerobic granular sludge: A review. *Process Saf. Environ. Prot.* **2022**, *163*, 27–35. [CrossRef]
36. Liu, X.; Dong, C. Simultaneous COD and nitrogen removal in a micro-aerobic granular sludge reactor for domestic wastewater treatment. *Syst. Eng. Procedia* **2011**, *1*, 99–105. [CrossRef]
37. Li, Y.Z.; He, Y.L.; Ohandja, D.G.; Ji, J.; Li, J.F.; Zhou, T. Simultaneous nitrification-denitrification achieved by an innovative internal-loop airlift MBR: Comparative study. *Bioresour. Technol.* **2008**, *99*, 5867–5872. [CrossRef] [PubMed]

38. Juang, Y.C.; Adav, S.S.; Lee, D.J.; Tay, J.H. Stable aerobic granules for continuous-flow reactors: Precipitating calcium and iron salts in granular interiors. *Bioresour. Technol.* **2010**, *101*, 8051–8057. [CrossRef]
39. Chen, Y.C.; Lin, C.J.; Chen, H.L.; Fu, S.Y.; Zhan, H.Y. Cultivation of Biogranules in a continuous flow reactor at low dissolved oxygen. *Water Air Soil Pollut. Focus* **2009**, *9*, 213–221. [CrossRef]
40. Wan, C.; Sun, S.; Lee, D.J.; Liu, X.; Wang, L.; Yang, X.; Pan, X. Partial nitrification using aerobic granules in continuous-flow reactor: Rapid startup. *Bioresour. Technol.* **2013**, *142*, 517–522. [CrossRef]
41. Beun, J.J.; Van Loosdrecht, M.C.M.; Heijnen, J.J. Aerobic granulation in a sequencing batch airlift reactor. *Water Res.* **2002**, *36*, 702–712. [CrossRef]
42. Vishniac, W.; Santer, M. The Thiobacilli. *Bacteriol. Rev.* **1957**, *21*, 195–213. [CrossRef] [PubMed]
43. Sguanci, S.; Lubello, C.; Caffaz, S.; Lotti, T. Long-term stability of aerobic granular sludge for the treatment of very low-strength real domestic wastewater. *J. Clean. Prod.* **2019**, *222*, 882–890. [CrossRef]
44. Liu, T.; He, X.; Jia, G.; Xu, J.; Quan, X.; You, S. Simultaneous nitrification and denitrification process using novel surface-modified suspended carriers for the treatment of real domestic wastewater. *Chemosphere* **2020**, *247*, 125831. [CrossRef] [PubMed]
45. Iannacone, F.; Di Capua, F.; Granata, F.; Gargano, R.; Esposito, G. Simultaneous nitrification, denitrification and phosphorus removal in a continuous-flow moving bed biofilm reactor alternating microaerobic and aerobic conditions. *Bioresour. Technol.* **2020**, *310*, 123453. [CrossRef] [PubMed]
46. Kiskira, K.; Papirio, S.; van Hullebusch, E.D.; Esposito, G. Influence of pH, EDTA/Fe(II) ratio, and microbial culture on Fe(II)-mediated autotrophic denitrification. *Environ. Sci. Pollut. Res.* **2017**, *24*, 21323–21333. [CrossRef] [PubMed]
47. APHA. *Standard Methods for the Examination of Water and Wastewater*; American Water Works Association: Denver, CO, USA; American Public Works Association: Kansas City, MI, USA; Water Environment Federation: Alexandria, VA, USA, 2005.
48. ISRA-CNR. *Analytical Methods for Water. Agenzia per la Protezione Dell'ambiente e per i Servizi Tecnici (APAT) Istituto di Ricerca Sulle Acque—Consiglio Nazionale Delle Ricerche*; ISRA-CNR: Rome, Italy, 2003; ISBN 8844800837.
49. Di Capua, F.; Mascolo, M.C.; Pirozzi, F.; Esposito, G. Simultaneous denitrification, phosphorus recovery and low sulfate production in a recirculated pyrite-packed biofilter (RPPB). *Chemosphere* **2020**, *255*, 126977. [CrossRef] [PubMed]
50. Bonomo, L. *Trattamenti Delle Acque Reflue*; McGraw-Hill: Milano, Italy, 2008; Volume 4, ISBN 9788838691645.
51. Qambar, A.S.; Al Khalidy, M.M. Optimizing dissolved oxygen requirement and energy consumption in wastewater treatment plant aeration tanks using machine learning. *J. Water Process Eng.* **2022**, *50*, 103237. [CrossRef]
52. Campano, E. idrico Piano d'Ambito Regionale. Available online: https://www.enteidricocampano.it/wp-content/uploads/2021/12/Relazione-PDA-Regionale_rev1_2021.pdf (accessed on 15 March 2023).
53. Show, K.Y.; Lee, D.J.; Tay, J.H. Aerobic granulation: Advances and challenges. *Appl. Biochem. Biotechnol.* **2012**, *167*, 1622–1640. [CrossRef]
54. Zhou, D.; Niu, S.; Xiong, Y.; Yang, Y.; Dong, S. Microbial selection pressure is not a prerequisite for granulation: Dynamic granulation and microbial community study in a complete mixing bioreactor. *Bioresour. Technol.* **2014**, *161*, 102–108. [CrossRef]
55. Campo, R.; Sguanci, S.; Caffaz, S.; Mazzoli, L.; Ramazzotti, M.; Lubello, C.; Lotti, T. Efficient carbon, nitrogen and phosphorus removal from low C/N real domestic wastewater with aerobic granular sludge. *Bioresour. Technol.* **2020**, *305*, 122961. [CrossRef]
56. Wang, X.; Wang, S.; Xue, T.; Li, B.; Dai, X.; Peng, Y. Treating low carbon/nitrogen (C/N) wastewater in simultaneous nitrification-endogenous denitrification and phosphorous removal (SNDPR) systems by strengthening anaerobic intracellular carbon storage. *Water Res.* **2015**, *77*, 191–200. [CrossRef]